Neuron, Vol. 31, 261–275, August 2, 2001, Copyright ©2001 by Cell Press

Neurotrophin-Induced Transport of a β-Actin mRNP Complex Increases β-Actin Levels and Stimulates Growth Cone Motility

H.L. Zhang,[1,4] T. Eom,[1,4] Y. Oleynikov,[2] S.M. Shenoy,[2] D.A. Liebelt,[1,2] J.B. Dictenberg,[1,2] R.H. Singer,[2] and G.J. Bassell[1,3]
[1] Department of Neuroscience
Rose F. Kennedy Center for Mental Retardation
Albert Einstein College of Medicine
Bronx, New York 10461
[2] Department of Anatomy and Structural Biology
Albert Einstein College of Medicine
Bronx, New York 10461

Summary

Neurotrophin regulation of actin-dependent changes in growth cone motility may depend on the signaling of β-actin mRNA transport. Formation of an RNP complex between the β-actin mRNA zipcode sequence and Zipcode Binding Protein 1 (ZBP1) was required for its localization to growth cones. Antisense oligonucleotides to the zipcode inhibited formation of this RNP complex in vitro and the neurotrophin-induced localization of β-actin mRNA and ZBP1 granules. Live cell imaging of neurons transfected with EGFP-ZBP1 revealed fast, bidirectional movements of granules in neurites that were inhibited by antisense treatment, as visualized by FRAP analysis. NT-3 stimulation of β-actin protein localization was dependent on the 3′UTR and inhibited by antisense treatment. Growth cones exhibited impaired motility in the presense of antisense. These results suggest a novel mechanism to influence growth cone dynamics involving the regulated transport of mRNA.

Introduction

Localization of specific mRNAs in neurons may provide an important mechanism to promote the enrichment of proteins at distinct subcellular sites and influence neuronal function (Tiedge et al., 1999; Kiebler and DesGrosiellers, 2000; Bassell and Singer, 2001). While considerable study has been devoted to understanding the implications of dendritic protein synthesis on synaptic function (Steward and Schuman, 2001), recent studies suggest that mRNA localization may also play a fundamental role in neuronal development during the period of axonal and dendritic outgrowth. The localization of mRNA and translational components has been observed as neurites begin to differentiate in culture (Bassell et al., 1994; Kleiman et al., 1994; Tiedge and Brosius, 1996). The localization of tau mRNA (Litman et al., 1993) and tropomyosin-5 mRNA (Hannan et al., 1995) into the incipient axon correlates with the enrichment and function of their cognate proteins in axonal growth and polarity.

[3] Correspondence: bassell@aecom.yu.edu
[4] These authors contributed equally to this work.

The localization of specific mRNAs and polyribosomes within growth cones may permit a direct response to external signals and rapidly influence cytoskeletal organization and outgrowth (Crino and Eberwine, 1997; Bassell et al., 1998). The localization of β-actin mRNAs to growth cones of minor neurites and the incipient axon correlated with the enrichment of β-actin protein to both types of growth cones (Bassell et al., 1998). The population of mRNAs present within growth cones was regulated by both age in culture and calcium (Crino and Eberwine, 1997). β-actin mRNAs localized rapidly to growth cones in response to NT-3, a response which required microtubules and cAMP-dependent protein kinase A (Zhang et al., 1999a). These studies suggest molecular interactions between *cis*-acting mRNA localization sequence(s) and *trans*-acting factors that are involved in regulation and cytoskeletal-dependent transport of mRNAs into developing processes and growth cones.

Specific mRNA-protein interactions that are involved in the regulation of mRNA transport within neurons are unknown. The present study was undertaken to examine the molecular mechanism and function underlying NT-3-regulated transport of β-actin mRNA in developing neurons. RNA-protein interactions required for β-actin mRNA trafficking to neuronal growth cones may bear similarity to the mechanism of mRNA localization to the leading edge of other motile cells. The localization of β-actin mRNA in fibroblasts was shown to involve a 54 nt sequence within the 3′UTR, termed the zipcode, that was sufficient and necessary for localization (Kislauskis et al., 1994). Using the 54 nt zipcode to identify specific RNA binding proteins by affinity purification, the RNA binding protein, Zipcode Binding Protein (ZBP1), was isolated and cloned (Ross et al., 1997). It is currently unknown whether the complex between ZBP1 and the β-actin zipcode is required for the cytoplasmic transport of β-actin mRNA in fibroblasts or neurons. In this study, we show that ZBP1 is expressed in neurons and that formation of an RNP complex is required for its dynamic trafficking into the neurite. We further demonstrate that an essential function of β-actin mRNA transport is to increase the local concentration of β-actin protein within growth cones and stimulate persistent forward movements in response to neurotrophin signals.

Results

Antisense Oligonucleotides to the β-Actin Zipcode Inhibit Localization of β-Actin mRNA to Growth Cones

We have previously described a starvation and stimulation paradigm to study the rapid signaling of β-actin mRNA localization to growth cones by NT-3 (Zhang et al., 1999a). We investigated whether antisense oligonucleotides to the 54 nt β-actin zipcode (Figure 1A) could inhibit this signaling. Antisense oligonucleotides were also used to a downstream 43 nt zipcode that was shown to have weak localizing activity (Kislauskis et al., 1994).

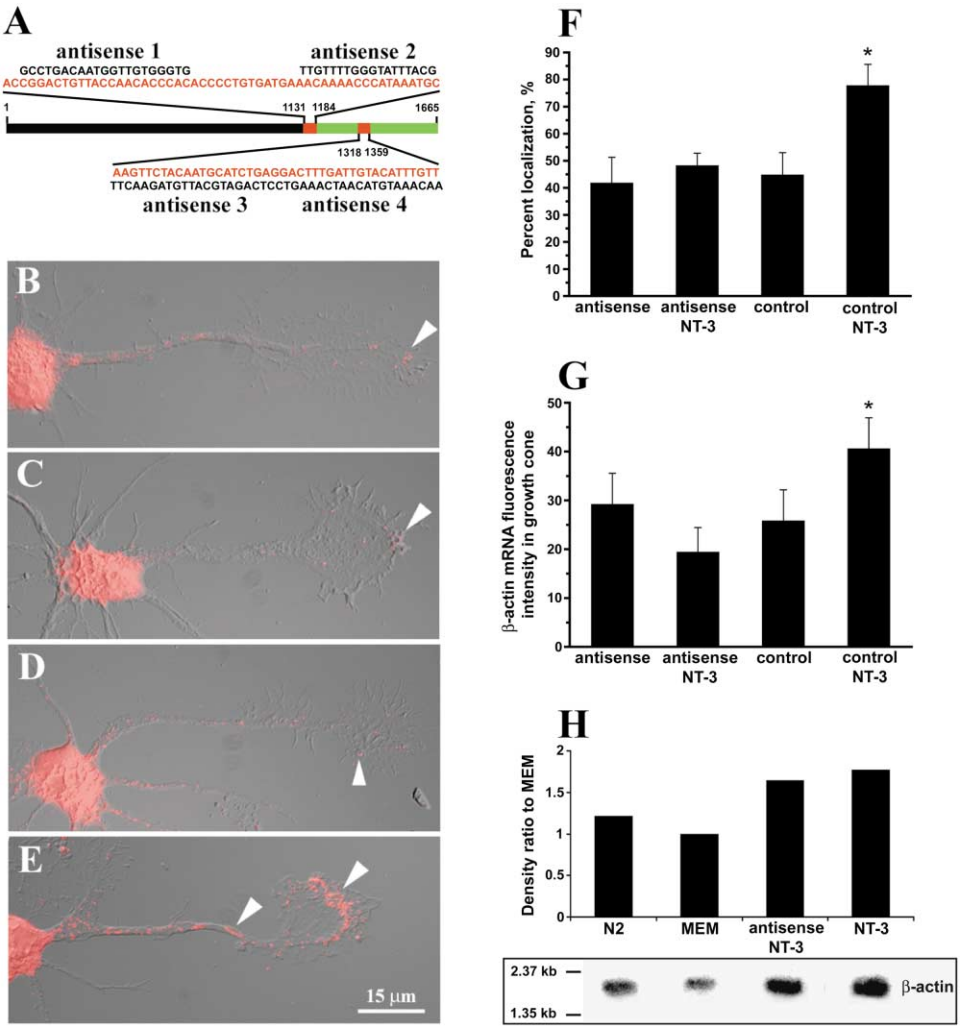

Figure 1. Antisense to β-Actin Zipcodes Inhibits Signaling of β-Actin mRNA Localization to Growth Cones by NT-3

(A) Schematic illustration showing the position of the 54 nt and 43 nt β-actin mRNA localization sequences (zipcodes) within the 3′UTR (Kislauskis et al., 1994). Two antisense oligonucleotides were designed to each of the zipcodes and used in combination. Coding region (black), 3′UTR (green), zipcodes (red).

(B–E) In situ hybridization to detect β-actin mRNA (red) in neurons that were starved or stimulated with NT-3 in the presence of antisense or reverse antisense oligonucleotides, as a control. Starved neurons did not show hybridization signal for β-actin mRNA in growth cones (B and D; arrows). Addition of NT-3 (25 ng/ml) to the starvation medium for 30 min in the presence of the antisense oligonucleotides failed to show β-mRNA localization in growth cones (C, arrow). In contrast, addition of NT-3 in the presence of the control oligonucleotides demonstrated strong signaling of β-mRNA localization to distal neurites and growth cones (E, arrows).

(F) The percentage of cells which exhibited β-actin mRNA within growth cones.

(G) The measurement of the fluorescence intensity (mean pixel intensity) of β-actin mRNA signal within growth cones. Both methods demonstrated a statistically significant increase in β-actin mRNA localization following NT-3 treatment, in the presence of the control oligonucleotides ($p < 0.01$, Student's t test).

(H) Northern Blot analysis of β-actin mRNA levels in normal culture conditions with N2 supplements, following starvation in MEM, 60 min in NT-3, with or without antisense treatment.

Cultured neurons were removed from their coculture with astrocytes in a supplemented media and starved in minimal essential medium (MEM) for three hours to delocalize the endogenous β-actin mRNA (Zhang et al., 1999a). Starved neurons were then treated with antisense (Figures 1B and 1C) or reverse antisense oligonucleotides, as a control (Figures 1D and 1E). Addition of antisense inhibited the signaling of β-actin mRNA localization in response to NT-3 treatment (Figure 1C). In contrast, control oligonucleotides did not block β-actin mRNA from localizing to growth cones in response to NT-3 (Figure 1E).

To quantitate these observations, we used two methods described previously (Zhang et al., 1999a). In the first method, starved neurons were visually scored as "localized" or "nonlocalized" for β-actin mRNA. The number of neurons localized was increased by 35% following NT-3 stimulation in the presence of the control oligonucleotides (Figure 1F). In contrast, there was not a significant change when the antisense oligonucleotides

were present during the NT-3 stimulation (Figure 1F). These data indicate an important role for the zipcode in the stimulation of β-actin mRNA localization by NT-3. The same observation was obtained when performing a statistical analysis of the average fluorescence intensity of the hybridization signal to β-actin mRNA within individual growth cones (Figure 1G). There was a 23% increase ($p < 0.01$) in the fluorescence intensity in stimulated neurons compared to starved neurons in the presence of the control oligonucleotides. There was no significant difference between the fluorescence intensities for probes hybridized to β-actin mRNA in starved neurons compared with neurons that were stimulated with NT-3 in the presence of the antisense oligonucleotides.

Northern blot analysis provided further support that antisense oligonucleotides to the β-actin zipcode had a direct effect on mRNA localization, and did not result in degradation or cleavage of β-actin mRNAs (Figure 1H). When neurons were starved in MEM, a reduction in total cell β-actin mRNA levels was observed. Stimulation of starved cells with NT-3 for 90 min resulted in an increase in β-actin mRNA levels (Figure 1H) irrespective of the presence or absence of antisense oligonucleotides. These observations indicated that despite the increase in β-actin mRNA levels following NT-3, the neurons were unable to localize these new β-actin mRNA transcripts in the presence of the antisense oligonucleotides.

Antisense Oligonucleotides to the β-Actin Zipcode Inhibit the Formation of an RNA-Protein Complex In Vitro

We postulated that antisense oligonucleotides disrupted β-actin mRNA localization by inhibiting the formation of a complex between the β-actin zipcode and a *trans*-acting factor that was necessary for the active transport of β-actin mRNA. The 54 nt β-actin zipcode was used to characterize a RNA-protein complex in vitro and study the effects of antisense oligonucleotide on complex formation. The zipcode formed a stable complex on nondenaturing gels that was not observed with a mutated sequence (Figure 2, left two lanes) (Ross et al., 1997). The formation of this zipcode-protein complex could be inhibited by competition with excess unlabeled zipcode (data not shown) or with increasing concentrations of antisense oligonucleotides (Figure 2A, middle lanes). A control oligonucleotide did not inhibit formation of the complex (Figure 2A, right three lanes). Therefore, the antisense inhibition of complex formation in vitro suggested that this interaction was required in vivo for β-actin mRNA localization.

ZBP1 Is Expressed in Forebrain Neurons and Forms a Complex with the β-Actin Zipcode

The RNA binding protein, Zipcode Binding Protein-1 (ZBP1), was isolated and cloned from chick embryo fibroblast cultures using affinity purification with the β-actin zipcode (Ross et al., 1997). We sought to determine whether ZBP1 was expressed in cultured forebrain neurons, and formed the RNA-protein complex with the β-actin zipcode. The expression of ZBP1 was demonstrated using RT-PCR and sequence analysis of poly (A) mRNA isolated from chick forebrain cultures (Figure 2B). Sequence analysis of the amplified PCR fragment (0.5 kb) showed that it was identical to the ZBP1 sequence from chick fibroblasts. Western blot analysis of chick forebrain cultures revealed the presence of a single band at the expected 66 kDa (Figure 2C) (Ross et al., 1997). Hence, the results of the RT-PCR, sequence analysis, and Western blot experiments indicated that ZBP1 was expressed in cultured chick forebrain neurons.

To determine whether ZBP1 was required for the formation of the RNP complex with the β-actin zipcode, the complex was crosslinked by UV irradiation and electrophoresed. This method permitted analysis of the approximate molecular weight of the RNA binding protein that had been UV-crosslinked. A single band was observed that migrated at the expected mobility (Figure 2D). To verify that this band corresponded to ZBP1, extracts were immunodepleted with anti-ZBP1 antibody or with preimmune serum. The supernatant was then incubated with the zipcode probe as above. Immunodepletion with the specific antibody, but not with preimmune serum, resulted in a substantial decrease in the amount of protein that was crosslinked to the zipcode (Figure 2E). These results indicate that ZBP1, expressed in forebrain cultures, forms an RNP complex with the β-actin zipcode.

ZBP1 and β-Actin mRNA Colocalize in Granules that Appear Coincident with Microtubules

To determine the spatial location of this RNP complex, ZBP1 and β-actin mRNA were visualized using double label in situ hybridization and immunofluorescence. We observed abundant distribution of ZBP1 and β-actin mRNA within the cell body, processes, and growth cones, and localized in the form of spatially distinct particles or granules (Figure 3A). Higher magnification revealed significant colocalization of the ZBP1 with β-actin mRNA (Figure 3A, a, b, and c).

Similar granules were observed when neurons were transfected with a ZBP1 fusion protein with enhanced green fluorescent protein (EGFP). EGFP-ZBP1 was abundant within the cell body, as was also observed for β-actin mRNA (Figure 3B). EGFP-ZBP1 and β-actin mRNA granules clustered together within the central domain of the growth cone (Figure 3B, lower arrows), whereas neither EGFP-ZBP1 nor β-actin mRNA was appreciable within the peripheral margin of the growth cone. Colocalization was also observed within the neurite (Figure 3B, upper white arrow). EGFP-ZBP1 could be observed within the neurite at sites devoid of β-actin mRNA (Figure 3B, white arrowhead). It is possible that the overexpression of EGFP-ZBP1 could promote formation of granules lacking in β-actin mRNA. Granules of β-actin mRNA were also observed at sites lacking EGFP-ZBP1 (Figure 3B, black arrow), although these granules may colocalize with the endogenous ZBP1. The EGFP vector lacking the ZBP1 insert, used as control, showed diffuse fluorescence within processes but did not reveal granules (not shown).

Previous work has shown that β-actin mRNA granules colocalized along microtubules within growth cones (Bassell et al., 1998). We investigated whether ZBP1 granules also displayed a similar association. ZBP1 and tubulin colabeling often revealed ZBP1 granules that

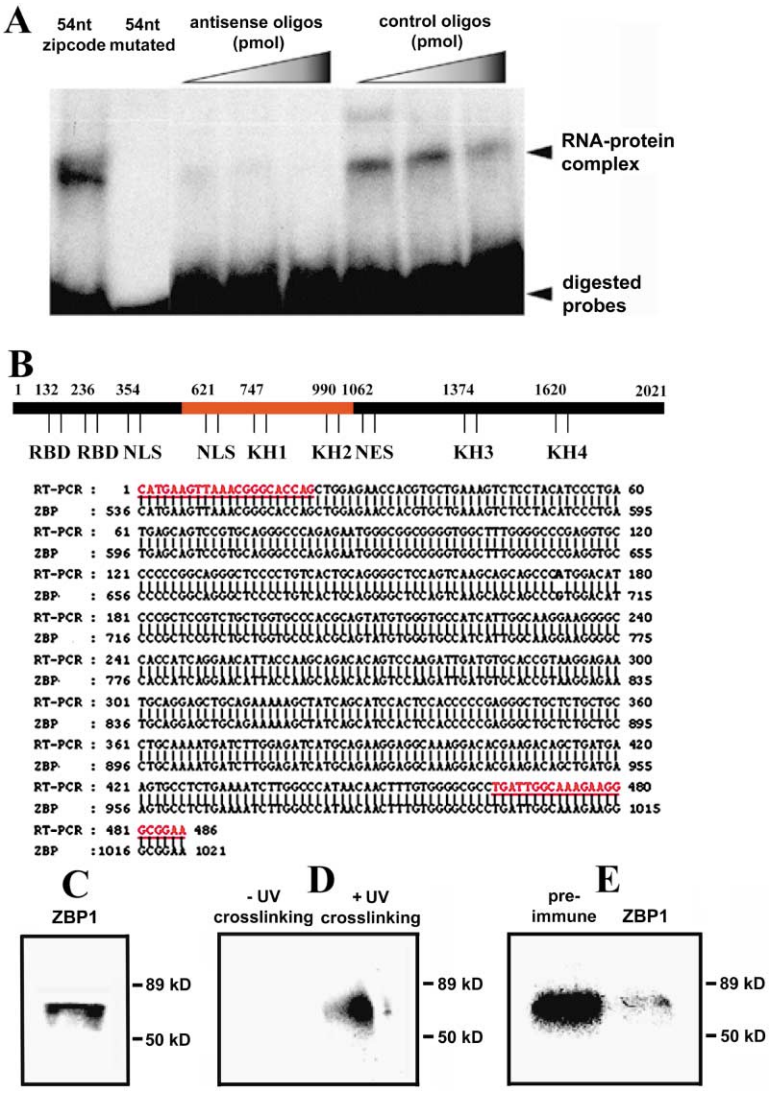

Figure 2. ZBP1 Forms an RNP Complex with the β-Actin Zipcode in Cultured Neurons

(A) A specific RNA-protein complex was observed with the 54 nt zipcode, but not with the 54 nt mutated zipcode (lanes 1 and 2). Formation of RNA-protein complexes with the β-actin zipcode was significantly inhibited by increasing concentration (from 1 to 5 pmol) of the antisense oligonucleotides, but not by the control oligonucleotides.

(B) Expression of ZBP1 in cultured forebrain neurons shown by RT-PCR and sequence analysis (within the amplified 486 nt sequence, red). RBD, RNA binding domain. NLS, nuclear localization sequence. KH, domain showing homology to hnRNP K.

(C) Western Blot analysis of chick forebrain cultures using anti-ZBP1 (VgRBP) antibody (Zhang et al., 1999c) showed a single band at approximately 66 kDa.

(D) UV crosslinking of neuronal culture extracts identified a protein of approximately 66 kDa that was bound to the ^{32}P-labeled zipcode.

(E) Immunodepletion of neuronal culture extracts with anti-ZBP1(VgRBP) antibody significantly reduced the formation of the RNA-protein complex with β-actin zipcode as in (D).

aligned along microtubules within growth cones (Figure 3C, arrowheads). These results suggest that ZBP1 and β-actin mRNA granules were present within neuronal processes and growth cones. The proximity of these granules to microtubules further suggests that this complex might be actively transported.

Fast Transport of ZBP1 Granules within Neuronal Processes

We investigated whether ZBP1 granules had dynamic behavior characteristic of fast transport. Live cell imaging revealed retrograde and anterograde movements of EGFP-ZBP1 granules (Figure 4). One of the many neurons imaged live is shown in Figure 4A . Two regions of interest are expanded (Figure 4B is Region I; 4C is Region II). Numerous motile ZBP1 granules, which varied in size, were observed within these processes (Figures 4B and 4C; blue and red arrows). We also observed a population of stationary or oscillatory particles (Figure 4B, white arrows). The oscillatory particles did not move in a specific net direction for a measurable distance, but exhibited short displacements within a small segmented area (<1 μm). We analyzed granules that moved in persistent anterograde or retrograde trajectories, for distances of at least a few microns (Figures 4B and 4C; blue and magenta arrows). A series of the individual frames is shown in Figures 4D and 4E to illustrate the movement of granules in Region I (Figures 4A and 4B), as an example (Quicktime movie can be viewed as Supplementary Material on the *Neuron* website, http://www.neuron.org/cgi/content/full/31/2/261/DC1).

Granule movements were analyzed in consecutive frames, and the instantaneous velocity for each granule was plotted over the time period the granule was tracked (Figure 4F). Six granules (from the thirteen shown in Figures 4A–4C) illustrated the different types of granule displacements and trajectories. Some granules moved persistently retrograde (Figure 4F: RI/G5) or anterograde (Figure 4F: RI/G7). Some granules moved in one direction, and paused for a prolonged period before resuming movement (Figure 4F: RI/G1). Bidirectional movement, both persistent and oscillatory, was also observed. These bidirectional granules often moved anterograde or retrograde and then reversed their direction (Figure

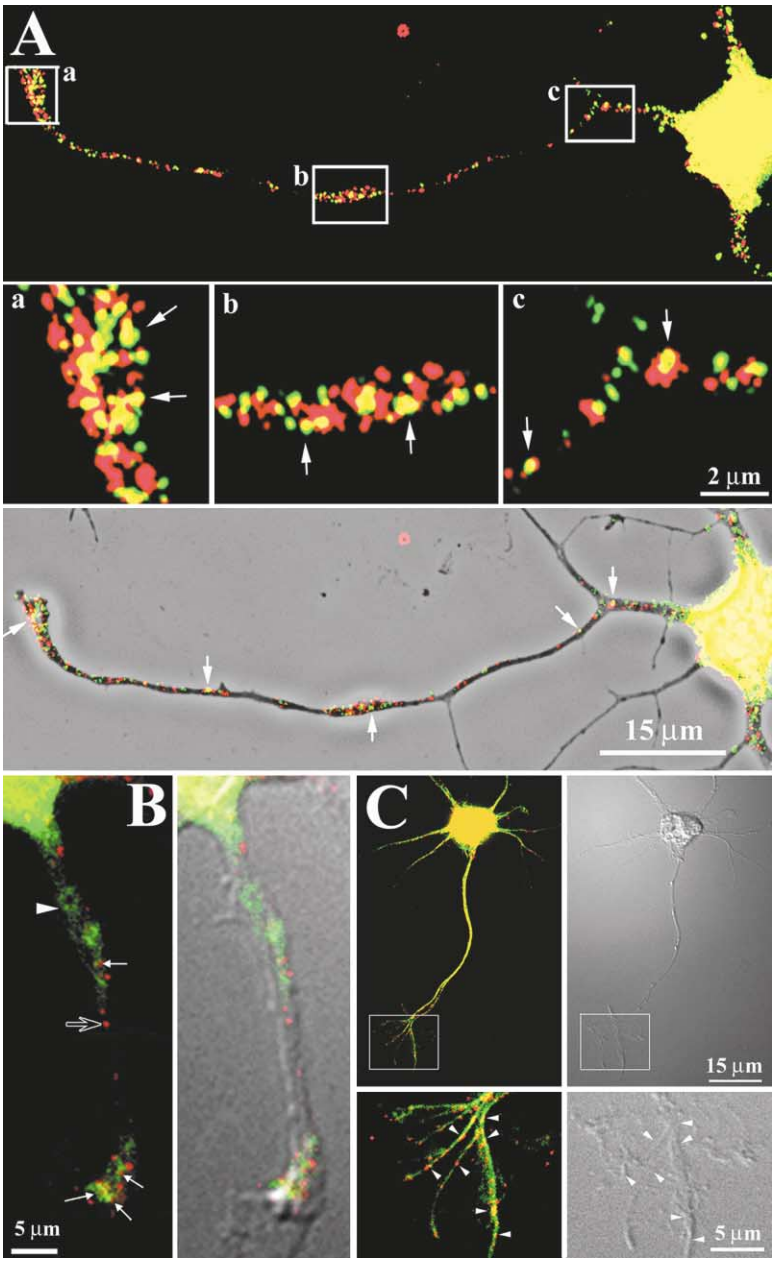

Figure 3. Localization of ZBP1 and β-Actin mRNA Granules within Neuronal Processes and Growth Cones

(A) ZBP1 (green) and β-actin mRNA (red) were localized within granules within neuronal processes and growth cones (top panel). Higher magnification of three regions (a, b, and c) showed colocalization of ZBP1 and β-actin mRNA within numerous granules (arrows). Phase optics are shown in lower panel.

(B) Neurons were transfected with EGFP-ZBP1 and fixed for in situ hybridization to β-actin mRNA (red). The overlaid images showed the colocalization or clustering of EGFP-ZBP1 with β-actin mRNA in the process and growth cone (arrows). EGFP-ZBP1 was also observed at sites that lacked β-actin mRNA signal (white arrowhead), as well as β-actin mRNA granules which had no apparent staining for EGFP-ZBP1 (black arrow). Right panel: overlay on DIC optics.

(C) ZBP1 granules delineate several microtubules, labeled with anti-tubulin (green), within the central domain of the growth cone (arrowheads in enlarged inset). Right panel: DIC optics.

4F: RI/G3, RII/G1). One granule (RII/G2) possessed both persistent and oscillatory bidirectional movements (Figures 4C and 4F). This granule moved both anterograde and retrograde and had brief irregular periods when it oscillated.

The mean instantaneous velocities ranged from 0.37 μm/s to 1.2 μm/s, and the average velocities ranged from 0.31 to 1.2 μm/s per granule. Other neurons imaged showed a comparable range of velocities (data not shown). There were no statistically significant differences between anterograde and retrograde rates. The anterograde distances ranged between 1.36 and 6.76 μm, and the retrograde distances were between 1.10 and 5.58 μm. These data demonstrate that ZBP1 granules exhibit dynamic anterograde and retrograde movements consistent with bidirectional fast transport.

Neurotrophin Regulation of ZBP1 Localization and Movement Is Inhibited by Antisense

The binding of ZBP1 to the β-actin zipcode may be necessary for the formation of an RNP complex that is actively transported into neuronal processes. Therefore, we hypothesized that antisense to the β-actin zipcode (which disrupts RNP complex formation) may prevent the localization of ZBP1 into processes. Accordingly, cultured neurons were subjected to starvation and subsequent stimulation in the presence of control or antisense oligonucleotides (see Figure 1). ZBP1 granules were delocalized by starvation and relocalized following NT-3 exposure. Antisense oligonucleotides inhibited the localization of ZBP1 granules to processes and growth cones in response to NT-3 stimulation of starved cells (Figures 5A and 5B). ZBP1 was largely confined to the

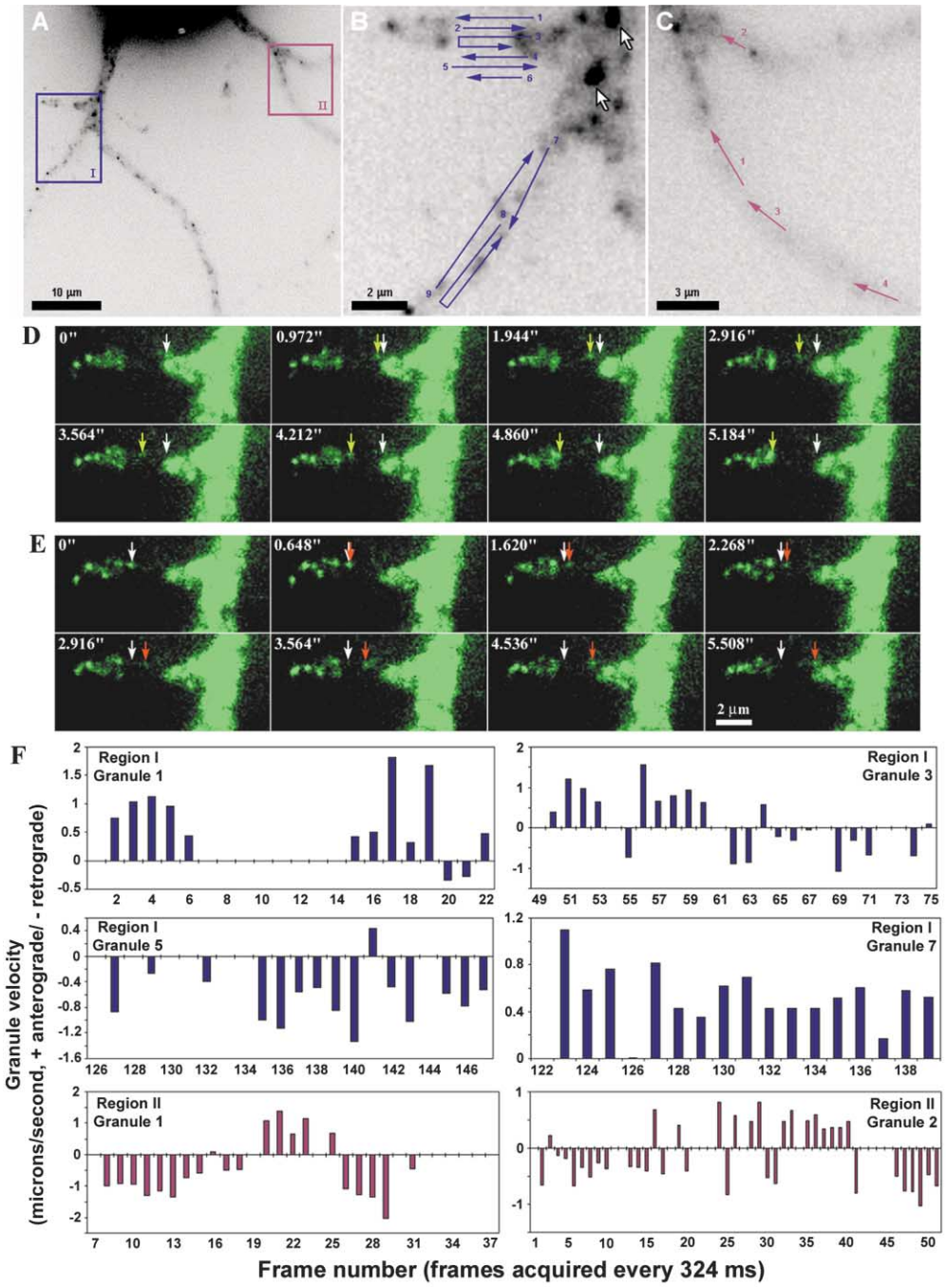

Figure 4. EGFP-ZBP1 Forms Granules which Exhibit Dynamic Anterograde and Retrograde Movements within Live Neurons

(A) EGFP-ZBP1 was observed in the form of granules (displayed in black) that were distributed throughout the neurites. Two regions of interest are indicated within blue (RI) and magenta (RII) boxes.

(B) Higher magnification view of RI. EGFP-ZBP1 granules were noted of varying sizes. The larger granules frequently were stationary or oscillatory, and accumulated at branch points or bifurcations between neurites (white arrows). The smaller granules were more motile, and exhibited dynamic anterograde and retrograde movements. Six motile granules were tracked in a short neurite which projected from the bifurcation (1–6, blue arrows; see also Quicktime movie as supplemental data on the *Neuron* website). Three other granules were tracked in an adjacent neurite (7–9, blue arrows). The arrows indicate the net direction of each trajectory.

(C) Higher magnification view of RII shows four granules (1–4, magenta arrows) that were tracked in a retrograde direction.

(D and E) Examples of EGFP-ZBP1 granule (shown in green) movements from (B) with high temporal resolution. (D) Granule 1, anterograde movement, white arrow indicates initial location, green arrow movement at depicted times. (E) Granule 2, retrograde movement, red arrow indicates movement at depicted times.

(F) EGFP-ZBP1 granules exhibiting bidirectional movements. Instantaneous velocities (between two consecutive frames) of each granule were plotted versus the time period that the granule could be tracked (movements of six granules are plotted).

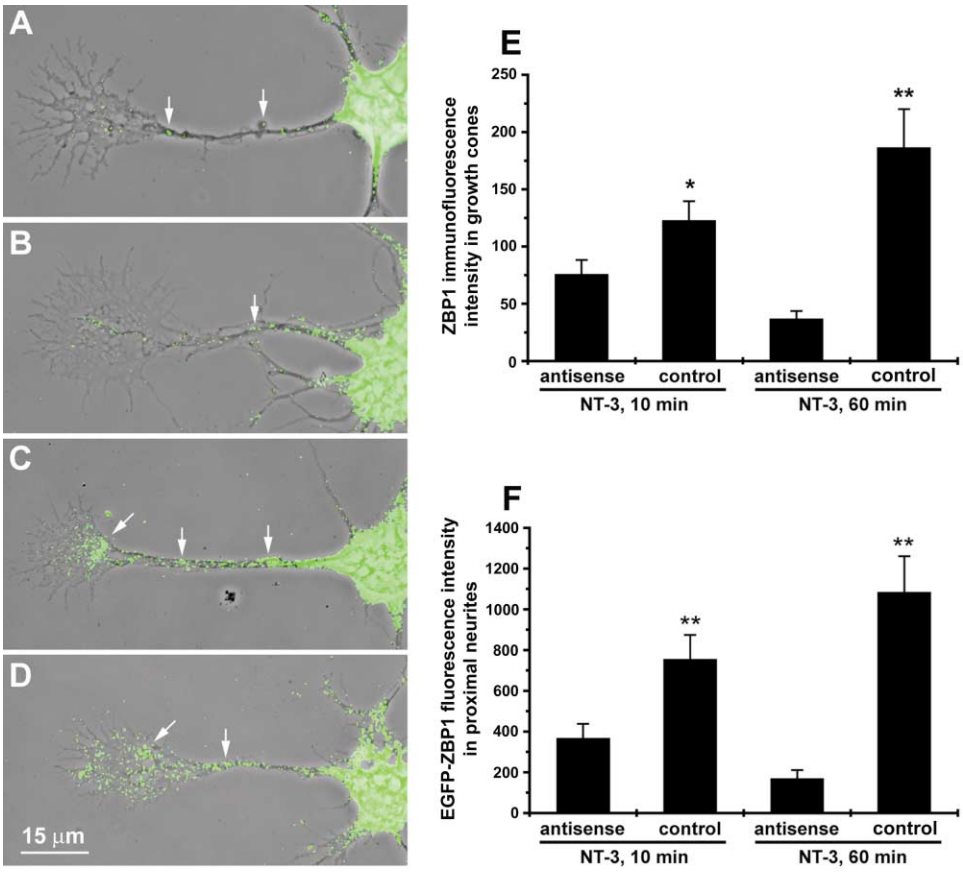

Figure 5. Antisense Oligonucleotides to the β-Actin Zipcode Inhibit the Localization of ZBP1

Cultured neurons were starved in MEM for 4 hr and then stimulated with NT-3 for 10 or 60 min in the presence of either antisense or control oligonucleotides. ZBP1 (green, detected by antibodies) was prominent in the cell body but not appreciable in distal neurites or growth cones after the starvation assay (not shown). Addition of NT-3 to the starvation medium for (A) 10 or (B) 60 min, in the presence of the antisense oligonucleotides, failed to show ZBP1 localization in distal segments and growth cones, although granules were observed within the proximal segment (arrows). In the presence of the control oligonucleotides, addition of NT-3 for (C) 10 or (D) 60 min demonstrated strong induction of ZBP1 localization to distal neurites and growth cones (arrows). (E) Quantitation of cells in (A)–(D) showed significantly higher fluorescence (pixel) intensities for ZBP1 in (C) and (D) than (A) and (B). (*, $p < 0.05$ for 10 min treatment; $p < 0.01$ for 1 hr treatment). (F) Cells transfected with EGFP-ZBP1 showed an increase in fluorescence intensities in proximal portion of the neurites with increased time in NT-3, in the presence of control oligonucleotides. As in (E), a reduction in ZBP1 fluorescence intensities was observed in the neurite over time when treated with antisense.

cell body, but was occasionally observed within the proximal segment of neurites (Figure 5B). ZBP1 levels within the proximal neurite were substantially higher in cells treated with control oligonucleotides (Figures 5C and 5D). Quantitative analysis of pixel intensities from both endogenous ZBP1 fluorescence (Figure 5E) and EGFP-ZBP1 transfection (Figure 5F) revealed reduced levels of ZBP1 within processes and growth cones following antisense exposure. The paucity of ZBP1 granules in distal neurites and growth cones was identical to that observed previously for β-actin mRNA localization following antisense treatment (Figure 1). These results indicate that inhibition of β-actin mRNA localization by antisense oligonucleotides also prevents the localization of ZBP1.

To more directly determine the effect of antisense treatment on ZBP1 kinetics, we used FRAP (fluorescent recovery after photobleaching) on EGFP-ZBP1 transfected neurons in the presence of antisense or control oligonucleotides (Figure 6). The rate of recovery after photobleaching an area within the neurite (see boxed area of cell in inset) was faster in the presence of the control oligonucleotides compared to the antisense. Representative neurites for each treatment show the recovery at $t = 60$ and $t = 300$ seconds after bleaching (Figures 6A–6H). The mean percent recovery at each time point was plotted for both control and antisense treatment (Figure 6I; $n = 8$ cells for each treatment). While cells treated with the reverse-antisense oligonucleotides recovered almost fully within 4 min (Figures 6A–6D and 6I), EGFP-ZBP1 localization in the presence of zipcode antisense barely reached 40% after 5 min (Figures 6E–6H and 6I). The calculated half-maximal time required for recovery was ~70 s for control treatment versus ~695 s for the antisense, almost a 10-fold difference in rate (see Experimental Procedures for calculation). The differences in kinetics were apparent even at early time points (Figures 6C and 6G; $t = 60$ s). Granules

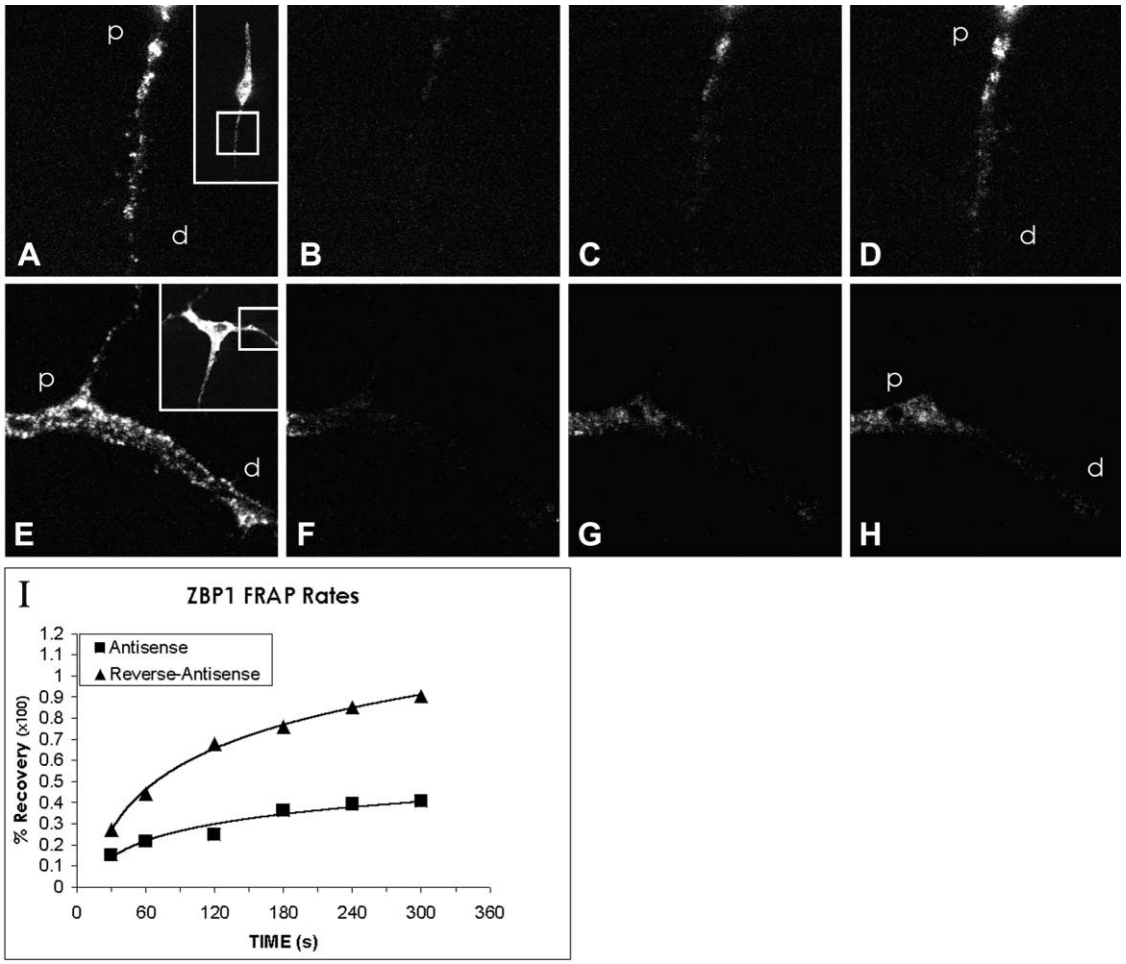

Figure 6. Effects of Zipcode Antisense on EGFP-ZBP1 Granule Movements into Photobleached Neurites Following NT-3 Stimulation

Cells were pretreated with either control (A–D) or antisense (E–H) oligonucleotides to the β-actin zipcode. Distribution of EGFP: (A and E) before photobleaching in a neurite that extends from cell body (inset), (B and F) immediately after photobleaching (t = 0), (C and G) 60 s, (D and H) 300 s. The neurite from the control treatment shows a rapid, almost full recovery of fluorescence whereas the neurite from the antisense treatment shows a slow, incomplete recovery of fluorescence. Granules moving into the neurite translocate more distal (d) in the control compared to the antisense, where they remain more proximal (p) to the cell body. (I) Time course of EGFP-ZBP1 translocation in either control (triangles) or antisense (squares) oligonucleotide-treated neurons.

entering the bleached zone generally moved more distally (see Figure 6D, d) into the neurite with control oligonucleotide treatment than did granules in the antisense-treated cells (see Fig. 6H, p). These results indicate that antisense oligonucleotides significantly reduced the motile fraction of ZBP1 in neurites, by approximately 60% compared to controls. Therefore, RNP complex motility may be regulated by the association of ZBP1 with the β-actin zipcode.

NT-3 Stimulation of β-Actin Protein Localization Is Dependent on the 3′UTR and Inhibited by Antisense

β-actin mRNA localization may provide a mechanism to locally elevate β-actin protein and promote growth cone protrusion. In order to determine whether β-actin protein levels within growth cones were reduced over time, following impaired β-actin mRNA localization, starved neurons were stimulated with NT-3 in the presence of antisense and the distribution of β-actin was assessed by immunofluorescence. Antisense treatment completely inhibited the stimulation of β-actin protein localization within growth cones in response to NT-3 (Figure 7A). In contrast, NT-3 stimulation in the presence of control oligonucleotides resulted in a 75% increase in β-actin protein content within growth cones compared to levels of starved neurons (Figure 7A). These results demonstrate that inhibition of β-actin mRNA localization has a direct effect on localized β-actin protein levels, presumably by reducing local synthesis of the β-actin isoform within growth cones.

Another approach to assess the role of the β-actin 3′UTR sequence in the localization of β-actin protein within growth cones was to transfect EGFP-β-actin fusion constructs with or without the zipcode and then analyze the concentration of EGFP-β-actin protein within growth cones. The presence of the β-actin 3′UTR resulted in a statistically significant increase in EGFP-β-

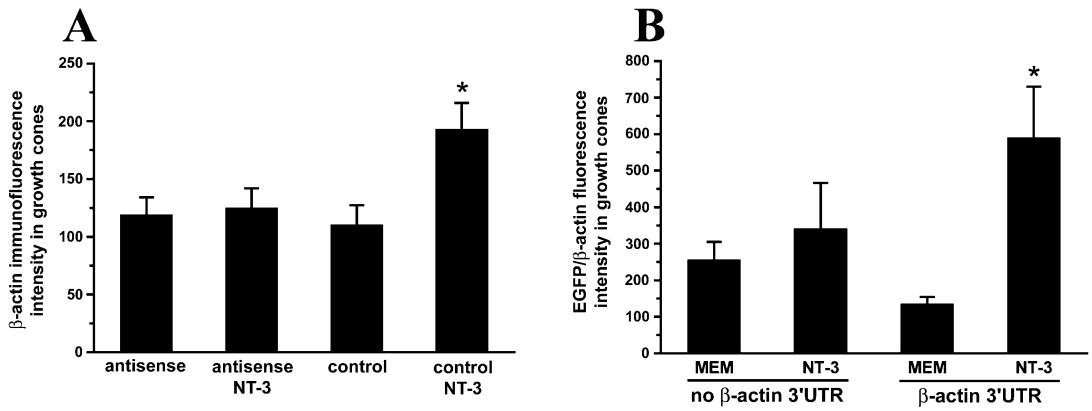

Figure 7. Concentration of β-Actin Protein within Growth Cones Following NT-3 Stimulation Is Dependent on Sequences within the β-Actin 3′UTR

(A) Neurons were starved for 3 hr and treated with NT-3 in the presence of antisense or control oligonucleotides for 90 min and then stained for β-actin by immunofluorescence. Antisense treatment inhibited the enrichment of β-actin protein within growth cones whereas the control treatment resulted in a 75% increase in the fluorescence intensity for β-actin protein (Student's t test: $p < 0.01$ when "control" group was compared to "control/NT-3" group).

(B) Neurons were transfected with β-actin-EGFP fusion constructs, with and without the β-actin mRNA 3′UTR, and then starved for 3 hr and treated with NT-3 for 90 min. Higher levels of β-actin-EGFP fluorescent intensity were observed within growth cones from the construct that contained the β-actin 3′UTR compared to the construct without the 3′UTR ($p < 0.01$).

actin fluorescence intensities in the growth cone (Figure 7B). In contrast, the 3′UTR deletion construct resulted in significantly lower EGFP-β-actin fluorescence intensities within growth cones following NT-3 treatment (Figure 7B). We have also obtained similar findings using epitope-tagged β-actin constructs where deletion of the β-actin zipcode from the 3′UTR reduced β-actin protein localization within growth cones (data not shown).

Retractive Behavior of Growth Cones with Reduced Levels of β-Actin mRNA and Protein

Growth cones with reduced levels of β-actin mRNA and protein would be expected to exhibit impaired movement in response to NT-3. Starved neurons were either treated with antisense or control oligonucleotides and then stimulated with NT-3 for 1 hr. Growth cone movements of live neurons were analyzed by time lapse phase microscopy. Growth cones treated with the control oligonucleotides exhibited persistent forward movements in response to NT-3 whereas growth cones from antisense treated cells exhibited predominantly retractive behavior (Figure 8).

To quantitate these observations, we used motion analysis software (see Experimental Procedures) to calculate the displacements of each growth cone over 60 consecutive frames within a time lapse. In Figure 8A, the mean displacement of the growth cone during the time lapse is shown for four antisense-treated cells and four control cells. Antisense-treated growth cones retracted at an average rate of −0.31 μm/min., whereas control growth cones moved forward at an average rate of 0.17 μm/min. (Figure 8A). The distance each growth cone moved during a 15 minute time course following NT-3 stimulation is plotted in Figure 8B. Growth cones treated with antisense exhibited persistent retractive displacement over time, whereas control-treated growth cones moved in a persistent forward direction. Before and after traces of growth cone shapes at initial and final time points within the time lapse are also presented (Figures 8C–8F). These data indicate that growth cones with reduced β-actin mRNA and protein levels exhibited impaired motility and dynamics in response to NT-3 stimulation.

Discussion

cis-Acting Elements and *trans*-Acting Factors Involved in Neuronal mRNA Localization

The results of our present study have demonstrated that the formation of a sequence-specific RNP complex between the β-actin zipcode and Zipcode Binding Protein (ZBP1) is required for mRNA transport within developing neurons. Other *cis*-acting sequences and possible *trans*-acting factors involved in mRNA localization within neurons have begun to be characterized. Sequences within the 3′UTR have been shown to be important for the dendritic localization of CaMKIIα mRNA (Mayford et al., 1996; Rook et al., 2000; Mori et al., 2000) and MAP2 mRNA (Blichenberg et al., 1999) and the localization of tau mRNA into the developing axon (Behar et al., 1995). Proteins have been isolated for their affinity to 3′UTR sequences within tau (Behar et al., 1995) and MAP2 mRNAs (Rehbein et al., 2000), although the identity and sequence of these proteins are unknown. In oligodendrocytes, the localization of myelin basic protein mRNA granules into processes was shown to involve a 21 nt RNA transport sequence (RTS) (Ainger et al., 1997) that is recognized by the RNA binding protein, hnRNP A2 (Hoek et al., 1998; Munro et al., 1999). The RTS was also shown to act as a translational enhancer (Kwon et al., 1999). Point mutations in the RTS that eliminated binding to hnRNPA2 were also impaired in mRNA transport (Munro et al., 1999). The use of antisense to knockdown

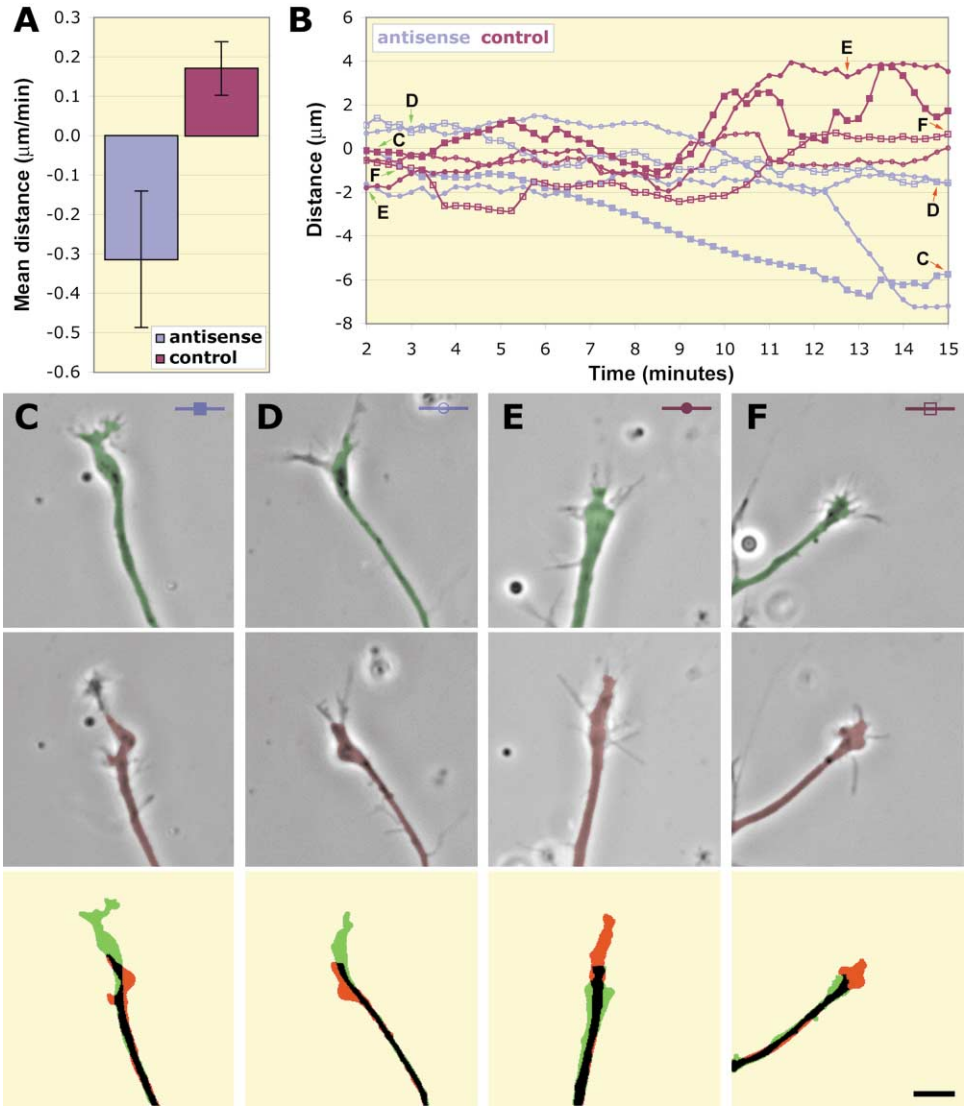

Figure 8. Retractive Behavior of Growth Cones Observed Following Zipcode Antisense Treatment

Starved neurons were either treated with antisense oligonucleotides to the β-actin zipcode or control oligonucleotides and then were stimulated with NT-3 for 1 hr. Forward movements were observed in control-treated growth cones, whereas antisense-treated growth cones exhibited retractive behavior. (A) Mean growth cone displacements (error bars indicate standard deviation, n = 4). Antisense-treated growth cones retracted at an average rate of −0.31 μm/min., whereas control growth cones moved forward at an average rate of 0.17 μm/min. (B) Individual growth cone displacements from (A) over time for antisense-treated cells (violet) and control cells (magenta). (C–F) Overlap illustrating the growth cone retraction from antisense-treated (C and D) or extension from control oligonucleotide-treated (E and F) cells (green = initial point, red = final point). The key in the upper right of each panel identifies each cell in (B). The initial and final time points for each frame are indicated by the triangles in (B). See also Quicktime movie as supplemental data on the *Neuron* website (http://www.neuron.org/cgi/content/full/31/2/261/DC1).

hnRNP A2 levels resulted in impaired transport of microinjected myelin basic protein mRNA (Ainger et al., 1997).

Active Transport of an mRNP Localization Complex in Neuronal Processes

Our observations are consistent with a trafficking function for ZBP1. ZBP1 and β-actin mRNA colocalized in granules within neuronal processes and growth cones. Inhibition of RNP complex formation between the β-actin zipcode and ZBP1, using antisense, decreased the localization of β-actin mRNA and ZBP1 into neurites and growth cones. FRAP analysis revealed a 10-fold reduction in ZBP1 movements into the neurite in the presence of antisense. While we were unable to directly assess the effects of antisense on the movements of β-actin mRNA in real time, owing to technical difficulties with microinjection of fluorescent zipcode sequences, the data presented do suggest a model in which the formation of an RNP localization complex is an essential step in the active transport of β-actin mRNA granules into the neurite. The interaction between ZBP1 and the β-actin zipcode may be necessary for subsequent binding to accessory factors, possibly motor molecules, as ZBP1

could be an adaptor between the mRNA and a motor. Further questions to address include whether interactions between the β-actin zipcode and ZBP1 are also important for mRNA anchoring or translation within growth cones once the mRNAs are localized.

The role of actin and microtubule-based motors in mRNA transport have begun to be elucidated in yeast and *Drosophila* oocytes, respectively (Long et al., 1997; Bertrand et al., 1998; Schnorrer et al., 2000; Brendza et al., 2000; Wilkie and Davis, 2001). In cultured fibroblasts, actin filaments (Sundell and Singer, 1991) and myosin IIB (Latham et al., 2001) are important mediators of regulated β-actin mRNA localization. However, in neurons, observations of an association of ZBP1 and β-actin mRNA (Bassell et al., 1998) and tau mRNA with microtubules (Litman et al., 1994) are more consistent with a microtubule-dependent transport mechanism. The mechanism of β-actin mRNA transport in neurons may bear similarity with oocytes, as the transport of Vg1 RNA to the vegetal cortex of *Xenopus* oocytes involves microtubules (Yisraeli et al., 1990), and the RNA binding protein, VgRBP or VERA, which happens to be the *Xenopus* homolog of ZBP1 (Elisha et al., 1995; Havin et al., 1998; Deshler et al., 1998). Conservation in localization mechanisms between oocytes and neurons was also evident by observations that rat tau mRNA sequences injected into oocytes localized to the vegetal cortex (Litman et al., 1996).

The fast bidirectional transport of a β-actin mRNA/ZBP1 complex in developing neurites at rates of 1 μm/s is analogous to the fast bidirectional transport of membrane bound vesicles and organelles (Hirokawa, 2000), suggesting possible involvement of both kinesin and dynein motors. Dynamic movements have also been described for other mRNA sequences or RNP complexes in neural cells. In oligodendrocyte processes, myelin basic protein mRNA granules move at a unidirectional rate of 0.2 μm/s, or oscillate at branch points (Ainger et al., 1993). The persistent unidirectional movements were dependent on microtubules and kinesin (Carson et al., 1997). RNA granules detected by the vital fluorescent dye, SYTO14, moved in anterograde and retrograde directions in neurites at rates of 0.1 μm/s (Knowles et al., 1996). The CaMKIIα 3′UTR coupled with GFP formed granules that exhibited oscillatory, unidirectional anterograde and unidirectional retrograde movements in hippocampal dendrites (Rook et al., 2000). The RNA binding protein, Staufen, when fused to GFP, exhibited granules that moved in dendrites at rates between 0.1–0.2 μm/s (Kohrman et al., 1999) and also associated with microtubules (Kiebler et al., 1999). Of interest, the rates for ZBP1 granules appear to be faster than Staufen, suggesting the possibility that different RNA binding proteins may be associated with different motors. The kinesin superfamily, for example, exhibits a wide range in rates and cargo binding characteristics (Hirokawa, 2000).

An important area of future work will be to understand how signal transduction pathways might influence dynamic bidirectional movements of mRNP complexes. Activation of trk receptors by NT-3 could result in phosphorylation of ZBP1 and subsequently promote the anterograde trafficking of ZBP1 into the neurite. It is possible that neurotrophin signaling could promote predominantly anterograde movements, possibly by affecting the balance between plus end- and minus end-directed movements of mRNA along microtubules. In support of this model, the distal translocation of SYTO14-labeled RNA granules was stimulated by the neurotrophin, NT-3 (Knowles and Kosik, 1997). Furthermore, KCl depolarization promoted an anterograde shift in the number of motile GFP-tagged CaMKIIα mRNA 3′UTR granules within dendrites (Rook et al., 2000). With regard to growth cones, the anterograde movements are likely involved in the delivery of β-actin mRNA from the cell body to the distal growth cone. We speculate that retrograde movements might be important to affect the redistribution of mRNA within the neurite, for example, by shifting sites of β-actin synthesis to filopodia or growth cones that sprout collateral branches. Retrograde movements may also relate to the possible function of ZBP1 as a shuttling protein (Y. Oleynikov et al., submitted) since it has putative nuclear localization and export sequences. Thus, a population of retrograde movements may reflect the transport of ZBP1 granules (without β-actin mRNA) back to the nucleus where it can complex with new β-actin mRNA transcripts.

Localization of β-Actin mRNA and Protein Affects Growth Cone Movement

Growth cone motility and directed outgrowth in response to extracellular signals, such as neurotrophins, are achieved by regulation of the actin cytoskeleton (Okada et al., 2000). The polymerization of actin within the growth cone is supported by an anterograde flux of actin monomer (Okabe and Hirokawa, 1991). The availability of actin monomers for polymerization may provide an important mechanism to regulate actin dynamics and growth cone motility. One means to deliver actin monomers to growth cones is by slow transport of a mobile, unassembled form of actin (Okada et al., 2000). The work presented here has indicated that another mechanism to influence local actin content within growth cones is to transport β-actin mRNA directly into neuronal processes. This view is consistent with previous analysis in fibroblasts that delocalization of β-actin mRNA can reduce cell migration and polarization (Kislauskis et al., 1997). β-actin mRNA localization would specifically concentrate the β-actin isoform, which has been suggested to be the preferred isoactin for the rearrangements of the actin cytoskeleton that occur in response to signaling at the membrane (Shuster and Herman, 1995; Bassell et al., 1998). β-actin could have higher binding affinities to actin binding proteins involved in de novo nucleation, uncapping, or severing of actin filaments. In support of this, disruption of cell polarity appears to be mediated through the localization of actin nucleation sites which are disrupted by antisense to the β-actin zipcode (Shestakova, et al., 2001).

It has been known that neurotrophins can act as long range chemoattractants and that actin dynamics underlie these directed movements (Gallo and Letourneau, 1998; Paves and Saarma, 1997). β-actin mRNA and consequent protein localization may specifically promote persistent forward movements of neurite growth cones. Altered regulation of β-actin mRNA localization could have dramatic consequences on the ability of a growth

cone to exhibit persistent directed movements in response to external signals. Instead of exhibiting persistent forward movements, in response to NT-3, the antisense-treated growth cones exhibited retractive behavior. Therefore, our work suggests that β-actin mRNA localization may be an essential downstream target of the neurotrophin signaling pathway, important for maintaining proper growth cone guidance and persistence of targeting. Further characterization of the mechanism involved in local β-actin synthesis and its effect on actin organization and dynamics will provide new insights into our understanding of the complex factors affecting growth cone motility. Likewise, the continued study of ZBP1 and its involvement in the microtubule-dependent transport of β-actin mRNAs and possibly other localized mRNAs will provide new insight into the function of mRNA transport as a novel mechanism to rapidly promote the sorting of cytoskeletal proteins within neuronal processes.

Experimental Procedures

Neuronal Culture, Neurotrophin Stimulation, and Antisense Treatment

We have previously described the use of primary cultures of embryonic chick forebrain as a model system to study β-actin mRNA localization within growth cones (Zhang et al., 1999a). Forebrain was dissected from 8-day chick embryos, trypsinized, dissociated, and plated on poly-L-lysine (0.2 mg/ml, 16 hr) and laminin (0.02 mg/ml, 12 min) coated coverslips in minimal essential medium (MEM) with 10% FBS for 2 hr. Cells were inverted onto a monolayer of astrocytes in N_2-conditioned medium with serum (2% FBS) and cultured for 4 days at 37°C in 5% CO_2. The cells were then fixed in paraformaldehyde (4% in PBS) at room temperature for 15 min.

We have previously described a starvation and stimulation assay to study the rapid signaling of β-actin mRNA localization to growth cones by NT-3 (Zhang et al., 1999a). This method involved removing the neurons from their coculture with astrocytes in a conditioned medium with N_2 supplements, and starving them in MEM for 4 hr, and then treated with NT-3 (25 ng/ml) (Austral Biologicals). Phosphorothioate-modified oligonucleotides were added to the MEM medium (12.5 μM each) for the last 2 hr of the starvation period. A mixture of four antisense oligonucleotides were used which were complementary to both the 54 nt and 43 nt zipcodes (Figure 1A) (Kislauskis et al., 1994). As a control, each of these sequences was synthesized in the reversed 5′–3′ orientation. Neurons were then stimulated with NT-3, in the presence of antisense or control oligonucleotides, for 10 to 90 min and then fixed.

In Situ Hybridization with Digoxigenin-Labeled Probes

Six amino-modified oligonucleotides (50 nt) complementary to 3′UTR sequences of chick β-actin mRNA were synthesized on a DNA synthesizer and chemically labeled using digoxigenin succinamide ester (Roche Molecular Biochemicals) as described previously. In situ hybridization for β-actin mRNA was completed as previously described (Bassell et al., 1998). The digoxigenin-labeled oligonucleotide probes were detected by immunofluorescence using Cy3-conjugated monoclonal antibody to digoxigenin and Cy3-conjugated anti-mouse antibody (Jackson Immunoresearch) as described previously (Zhang et al., 1999a). Coverslips were mounted with gelvatol with n-propyl gallate (6 mg/ml) as an anti-bleaching agent.

Immunofluorescence

For detection of endogenous proteins, we used monoclonal antibodies to β-actin and tubulin (Sigma), rabbit anti-VgRBP antibody (provided by Nancy Standart) (Zhang et al., 1999c), rabbit anti-HCC antibody (provided by Eng Tan) (Zhang et al., 1999b), and rabbit anti-ZBP1 antibody. All secondary antibodies were affinity-purified donkey antibodies to mouse or rabbit IgG conjugated to a fluorochrome (Jackson Immunoresearch). Antibody incubations were for 1 hr at room temperature in Tris-buffered saline (TBS) with BSA (1%) and Triton X-100 (0.1%). Coverslips were mounted with gelvatol with n-propyl gallate (6 mg/ml) as an anti-bleaching agent.

Fluorescence Microscopy and Quantitative Digital Imaging

Cells were viewed with a Nikon Eclipse inverted microscope equipped with a 60× Plan-Neofluar objective, phase optics, 100 W mercury arc lamp, and HiQ bandpass filters (ChromaTech). Images were captured with a cooled CCD camera (Quantix, Photometrics) using a 35 mm shutter and processed using IP Lab Spectrum (Scanalytics). Growth cones were selected randomly using phase optics and a fluorescence image of β-actin mRNA (in situ hybridization), β-actin protein, or ZBP1 (immunofluorescence) was then acquired. Exposure times were kept constant and below gray scale saturation. Quantitative analysis for mRNA and protein localization within growth cones was analyzed using fluorescence (pixel) intensities within growth cones as described previously (Zhang et al., 1999a). The perimeter of 10 to 30 growth cones, for each experimental variable, were first traced from the phase image using IP Lab software to identify a region of interest (ROI). The total fluorescence intensity was then divided by area to obtain mean pixel intensity. For quantitative analysis of β-actin mRNA localization using a visual scoring method, 100 cells per coverslip were analyzed for each cell culture condition. Cells were scored as "localized" if several granules were observed, and scored as "nonlocalized" if the signal was not distinguishable from background levels (hybridization with control probe).

EGFP-ZBP1 Transfections and Live Cell Imaging

The chick ZBP1 coding sequence (Ross et al., 1997) was inserted into the downstream cloning site of Enhanced Green Fluorescence Protein (EGFP) in the pEGFP-C1 expression vector with a CMV promoter (Clonetech) and transfected into freshly dissociated forebrain neurons using the lipid reagent, DOTAP (Boehringer Manheim) (Kaech et al., 1996). Neurons were plated on poly-L-lysine and laminin coated coverslips in the presence of 10% FBS for 2 hr, transferred to N2 media, and cultured for 4 days as described above. Coverslips were transferred to a sealed environmental chamber (Bioptechs Focht Chamber) in Leibovitz L-15 medium (Gibco BRL) with N2 supplements in order to maintain CO_2. Imaging of live neurons was performed using a TILL Photonics Imaging System with a Polychrome II monochromator and high resolution Imago CCD camera. Cells were imaged at an exposure rate of 0.324 s for each frame.

A 200-frame stack was acquired (resolution of 111.7 nm/pixel) and was inverted and scaled with NIH Image (Scion Image). A macro was written which outputs the x and y coordinates of the granule centroid and the frame number into a tab-delimited text file which was used in Microsoft Excel to calculate granule velocities between frames.

Fluorescence recovery after photobleaching (FRAP) analysis of EGFP-ZBP1 was done on cultured forebrain neurons subjected to the starvation/stimulation paradigm using NT-3. Images were captured (488 nm excitation) using a laser scanning confocal microscope (BioRad Radiance 2000). Transfected cells were randomly selected and subregions of the neurite, usually the proximal segment, were bleached with full intensity laser until the EGFP signal was almost fully eliminated (~30 s). Recovery was imaged at low laser power, and cells were examined for 5 min, imaging every 10 s. Percent recovery was determined by subtracting arbitrary average background values outside the cell from average values from the whole neurite or selected subregions from within the neurite at any given time point, then dividing this by the difference in fluorescence intensity of the selected region before bleaching and the average background values $(I_{spot} - I_{bkgd}(\text{post-bleach})/I_{spot} - I_{bkgd}$ (pre-bleach). Each of the traces was calculated from an average percent recovery of $n = 8$ cells at each time point, starting at 30 s post bleach. Half-maximal time points for each treatment were calculated by using the regression equations derived from the best-fit curve of the recovery time points and calculating for 50% recovery ($y = 0.5$). A similar approach has been used to measure translocation kinetics of CaMKII subunits in dendrites (Shen and Meyer, 1999).

Live Cell Imaging of Growth Cone Motility Following Antisense Treatment

Coverslips were transferred to a closed chamber (Bioptechs Focht Chamber) following the starvation/stimulation paradigm in the presence of either antisense or control oligonucleotide and NT-3 stimulation for 1 hr as described above. Time lapse microscopy was performed using a cooled CCD camera (Quantix, Photometrics) and IP Lab software. Each growth cone was randomly selected and imaged for 15 min following NT-3 application. Four frames were acquired each minute for a total of 60 frames. Growth cone displacement was defined as the distance traversed by the distal edge of the growth cone palm in each frame of the time lapse sequence and analyzed automatically using a script written within IPLab software that measured optical density and morphometric characteristics of the growth cone. The signal from filopodia was eliminated by differential thresholding as they contributed excessive fluctuations in the analysis. Displacement was measured along a straight line extended from a line best fit to the cylindrical axis of the 10 to 15 μm portion of the neurite closest to the growth cone in the first frame of the time lapse sequence.

Transfection of EGFP-β-Actin Fusion Constructs

Full-length chick β-actin cDNA or a 3′UTR deletion construct (Kislauskis et al., 1994) were subcloned into the C terminus of EGFP in the pEGFP-C1 vector (Clonetech) and were transfected into freshly dissociated forebrain neurons using DOTAP as described above. Cells were plated onto poly-L-lysine and laminin coated coverslips in the presence of 10% FBS for 2 hr, transferred to N2 media, cultured for 4 days, and then subjected to the starvation/stimulation paradigm as described. The fluorescence intensity for EGFP-β-actin was analyzed in traced growth cones using the method described for immunofluorescence with the β-actin antibody (discussed above).

RT-PCR Amplification of ZBP1 mRNA

Total RNA from chick neuronal cultures was isolated using Tri Reagent (Molecular Research) and reverse transcribed using oligo$(dT)_{12\text{-}18}$ with M-MLV reverse transcriptase (Gibco BRL). PCR was performed for 35 cycles with sense and antisense primers designed from the chick ZBP1 sequence (Ross et al., 1997).

Electrophoretic Mobility Shift Assay (EMSA)

Cultured neurons were washed twice in (1× PBS, on ice) and scraped in cold buffer A (0.5 mM PMSF, 0.5 μg/ml leupeptin, 1 μg/ml aprotinine, 1× PBS). Cells were centrifuged for 5 min at 1,500 × g and resuspended in lysis buffer (50 mM Tris/HCl [pH 8.0], 100 mM NaCl, 0.5 mM dithiothreitol (DTT), 3 mM $MgCl_2$, 0.5 mM PMSF, 0.5 μg/ml leupeptin, 1 μg/ml aprotinine,1% Triton X-100). Cells were extracted for 30 min on ice and centrifuged for 10 min at 1,500 × g at 4°C, and supernatants were collected and pooled.

^{32}P-labeled RNA probes were transcribed in vitro from Ava I-linearized pSP64 construct of the β-actin 54 nt zipcode and a mutated zipcode using SP6 RNA polymerase (Promega) and 50 μCi of [α-^{32}P] CTP (Amersham) for 1 hr at 37°C. RNA was purified by denaturing gel electrophoresis. Radiolabeled RNA probes (50,000 cpm/μl) were incubated with pooled protein extracts from cultured forebrain neurons (20–40 μg) for 20 min at room temperature in binding solution (20 mM HEPES [pH 7.6], 3 mM $MgCl_2$, 100 mM KCl, 2 mM DTT, and 5% glycerol). Unbound RNA was digested with RNase T1 (1U) (Gibco BRL), and nonspecific RNA-protein interactions were minimized by incubation with heparin (5 mg/ml). RNA-protein complexes were resolved in a nondenaturing 4% polyacrylamide native gel and visualized by autoradiography. Competition assays were performed by preincubation of the protein extract with unlabeled RNA competitors for 10 min at room temperature before the radiolabeled RNA was added. Antisense (GCATTTATGGGTTTTGTT/GTGGGTGTTGGTAA CAGTCCG) or control oligonucleotides (TTGTTTTGGGTATTTACG/ GCCTGACAATGGTTGTGGGTG) were incubated with the radiolabeled RNA probes, for 10 min at 50°C, prior to incubation with neuronal extracts. The amount of the antisense oligonucleotide ranged from 1.0 to 5.2 pmol.

UV Crosslinking and Immunodepletion Assay

RNA-protein complexes were first formed as described above, exposed to UV light (GS Genelinker, Bio-Rad) at a distance of 2 cm for 8 min, digested with RNase T1 (1U, 10 min), and incubated with heparin (5 mg/ml, 10 min). ^{32}P-labeled RNA-protein complexes were first resolved in a nondenaturing 4% polyacrylamide native gel and visualized by autoradiography. Radiolabeled bands were excised, incubated in SDS sample buffer (2 hr, at 37°C), analyzed by 10% SDS-PAGE, and labeled proteins were detected by autoradiography.

For the immunodepletion assay, antibodies (10 μl) against ZBP1 (VgRBP) (Zhang et al., 1999c) were incubated (2 hr at 4°C) with neuronal culture extracts (20 μl) with gentle agitation. Protein A-agarose (Roche Molecular Biochemicals) suspension was added to a mixture of neuronal extracts and antibody complexes and incubated overnight (4°C). Complexes were centrifuged (12,000 × g, 20 s) and the supernatant was incubated with radiolabeled RNA (20 min at room temperature) and UV crosslinked as above.

Western Blot

Neuronal culture extracts (10 μl) were resolved by 12% SDS-PAGE, and fractionated proteins were transferred to Hybond ECL nitrocellulose membrane (Amersham) at 4°C overnight. ZBP1 was detected with rabbit antibody to VgRBP (Zhang et al., 1999c) at 1:1000 in PBS with 1% BSA. The membrane was washed and incubated with peroxidase-conjugated goat anti-rabbit IgG (Jackson Immunoresearch) and the signal developed using ECL detection reagents (Amersham).

Northern Blot

Total cellular RNA was isolated from chick forebrain cultures using Tri Reagent (Molecular Research Center) and dissolved in DEPC-treated distilled water. RNA (8 μg) was electrophoresed in 0.8% formaldehyde-denatured agarose gel and transferred to Zeta-probe blotting membrane (Bio-Rad). The cDNA fragments (372 bp) complementary to the β-actin mRNA reading frame sequence were labeled with ^{32}P-dCTP (Amersham) using Random Primers DNA Labeling System (Gibco-BRL) and purified with Quick Spin columns (Boehringer Mannheim). The RNA binding membrane was hybridized in 5×SSPE supplemented with 1× Denhardt's, 0.2% SDS, 10% dextran sulfate, 100 μg/ml salmon testes DNA, and 50% formamide with ^{32}P-labeled cDNA probes at 45°C overnight. After washes, the membrane was exposed to X-ray film (Kodak). Bands on the exposure film were scanned using a densitometer (Molecular Dynamics) and the optical densities were analyzed quantitatively using ImageQuant software.

Acknowledgments

We thank Suzanne Zukin for helpful discussions and suggestions on this manuscript. We thank Kim Farina, Nancy Standart, and Eng Tan for providing antibodies to ZBP, VgRBP, and HCC. We thank Adam Hartley for assistance with figure preparation and Jeff Levsky for assistance with computer programming. This work was supported by the National Science Foundation grant IBN9811384 and National Institutes of Health (NIH) RO1 grants GM55599 and NS39641 to G.J.B. and AR41480 to R.H.S. This work was also supported by the Muscular Dystrophy Foundation awards to H.L.Z. and G.J.B. H.L.Z. was supported by NIH training grant (T32 NS07439). J.B.D. was supported by NIH training grant (CA09475-13) and is the recipient of the Albert Einstein Scholar Award.

Received August 30, 2000; revised May 23, 2001.

References

Ainger, K.A., Avossa, D., Morgan, F., Hill, S.J., Barry, C., Barbarese, E., and Carson, J.H. (1993). Transport and localization of exogenous myelin basic protein mRNA microinjected into oligodendrocytes. J. Cell Biol. *123*, 431–441.

Ainger, K.A., Avossa, D., Diana, A.S., Barry, C., Barbarese, E., and Carson, J.H. (1997). Transport and localization elements in MBP mRNA. J. Cell Biol. *138*, 1077–1087.

Bassell, G.J., and Singer, R.H. (2001). Neuronal RNA localization and the cytoskeleton. In Results and Problems in Cell Differentiation, D. Richter, ed. (Berlin: Springer-Verlag), pp. 41–56.

Bassell, G.J., Singer, R.H., and Kosik, K.S. (1994). Association of poly(A) mRNA with microtubules in cultured neurons. Neuron *12*, 571–582.

Bassell, G.J., Zhang, H.L., Byrd, A.L., Femino, A.M., Singer, R.H., Taneja, K.L., Lifshitz, L.M., Herman, I.M., and Kosik, K.S. (1998). Sorting of β-actin mRNA and protein to neurites and growth cones in culture. J. Neurosci. *18*, 251–265.

Behar, L., Marx, R., Sadot, E., Barg, J., and Ginzburg, I. (1995). cis-Acting signals and trans-acting proteins are involved in tau mRNA targeting into neurites of differentiating neuronal cells. Int. J. Dev. Neurosci. *13*, 113–127.

Bertrand, E., Chartrand, P., Schaefer, M., Shenoy, S.M., Singer, R.H., and Long, R.M. (1998). Localization of ASH1 RNA particles in living yeast. Mol. Cell *2*, 437–445.

Blichenberg, A., Schwanke, B., Rehbein, M., Garner, C.C., Richter, D., and Kindler, S. (1999). Identification of a cis-acting dendritic targeting element in MAP2 mRNAs. J. Neurosci. *19*, 8818–8829.

Brendza, R.P., Serbus, L.R., Duffy, J.B., and Saxton, W.M. (2000). A function for kinesin I in the posterior transport of oskar mRNA. Science *289*, 2120–2122.

Carson, J.H., Worboys, K., Ainger, K., and Barbarese, E. (1997). Translocation of MBP mRNA in oligodendrocytes requires microtubules and kinesin. Cell Motil. Cytoskel. *38*, 318–328.

Crino, P.B., and Eberwine, J. (1997). Molecular characterization of the dendritic growth cone. Neuron *17*, 1173–1187.

Deshler, J.O., Highett, M.I., and Schnapp, B.J. (1998). A highly conserved RNA binding protein for cytoplasmic mRNA localization in vertebrates. Curr. Biol. *8*, 489–496.

Elisha, Z., Havin, L., Ringel, I., and Yisraeli, J.K. (1995). Vg1 RNA binding protein mediates the association of Vg1 RNA with microtubules in Xenopus oocytes. EMBO J. *14*, 5109–5114.

Gallo, G., and Letourneau, P. (1998). Localized sources of neurotrophins initiate axon collateral sprouting. J. Neurosci. *18*, 5403–5414.

Hannan, A.J., Schevzov, G., Gunning, P., Jeffrey, P.L., and Weinberger, R.P. (1995). Intracellular localization of tropomyosin mRNA and protein is associated with development of neuronal polarity. Mol. Cell. Neurosci. *6*, 397–412.

Havin, L., Git, A., Elisha, Z., Oberman, F., Yaniv, K., Schwartz, S.P., Standart, N., and Yisraeli, J.K. (1998). RNA binding protein conserved in both microtubule and microfilament based RNA localization. Genes Dev. *12*, 1593–1598.

Hirokawa, N. (2000). Kinesin and dynein superfamily proteins and the mechanism of organelle transport. Science *279*, 519–526.

Hoek, K.S., Kidd, G.J., Carson, J.H., and Smith, R. (1998). hnRNPA2 selectively binds the cytoplasmic transport sequence of MBP mRNA. Biochem. *37*, 7021–7029.

Kaech, S., Kim, J.B., Cariola, M., and Ralston, E. (1996). Improved lipid mediated gene transfer into primary cultures of hippocampal neurons. Mol. Brain Res. *233*, 66–69.

Kiebler, M.A., and DesGroseillers, L. (2000). Molecular insights into mRNA transport and local translation in the mammalian nervous system. Neuron *25*, 19–28.

Kiebler, M.A., Hemraj, I., Verkade, P., Kohrman, M., Fortes, P., Marion, R.M., Ortin, J., and Dotti, C.G. (1999). The mammalian Staufen protein localizes to the somatodendritic domain of cultured hippocampal neurons: implications for its involvement in mRNA transport. J. Neurosci. *19*, 288–297.

Kislauskis, E.H., Zhu, X., and Singer, R.H. (1994). Sequences responsible for intracellular localization of β-actin messenger RNA also affect cell phenotype. J. Cell Biol. *127*, 441–451.

Kislauskis, E.H., Zhu, X., and Singer, R.H. (1997). Beta-actin messenger RNA localization and protein sythesis augment cell motility. J. Cell Biol. *136*, 1263–1270.

Kleiman, R., Banker, G., and Steward, O. (1994). Development of subcellular mRNA compartmentation in hippocampal neurons in culture. J. Neurosci. *14*, 1130–1140.

Knowles, R.B., and Kosik, K.S. (1997). Neurotrophin-3 signals redistribute RNA in neurons. PNAS *94*, 14804–14808.

Knowles, R.B., Sabry, J.H., Martone, M.E., Deerinck, T.J., Ellisman, M.H., Bassell, G.J., and Kosik, K.S. (1996). Translocation of RNA granules in living neurons. J. Neurosci. *16*, 7812–7820.

Kohrman, M., Lui, M., Kaether, C., DesGroseillers, L., Dotti, C.G., and Kiebler, M.A. (1999). Microtubule dependent recruitment of Staufen-GFP into large RNA containing granules and dendritic transport in living hippocampal neurons. Mol. Biol. Cell *10*, 2945–2953.

Kwon, S., Barbarese, E., and Carson, J.H. (1999). The cis-acting RNA trafficking signal from myelin basic protein mRNA and its cognate trans-acting ligand hnRNP A2 enhance cap-dependent translation. J. Cell Biol. *147*, 247–256.

Latham, V.L., Jr., Yu, E.H.S., and Tullio, A., Adelstein, R.S., and Singer, R.H. (2001). A rho-dependent signaling pathway operating through myosin localizes β-actin mRNA in fibroblasts. Curr. Biol. *11*, 1010–1016.

Litman, P., Barg, J., Rindzoonski, L., and Ginzburg, I. (1993). Subcellular localization of tau mRNA in differentiating neuronal cell culture: Implications for neuronal polarity. Neuron *10*, 627–638.

Litman, P., Barg, J., and Ginzburg, I. (1994). Microtubules are involved in the localization of tau mRNA in primary neuronal cultures. Neuron *13*, 1463–1474.

Litman, P., Behar, L., Elisha, Z., Yisraeli, J.K., and Ginzburg, I. (1996). Exogenous tau mRNA is localized in oocytes: possible evidence for evolutionary conservation of localization mechanisms. Dev. Biol. *176*, 84–94.

Long, R.M., Singer, R.H., Meng, X., Gonzalez, I., Nasmyth, K., and Jansen, R.P. (1997). Mating type switching in yeast controlled by asymmetric localization of ASH1 mRNA. Science *277*, 383–387.

Mayford, M., Baranes, D., Podsypanina, K., and Kandel, E.R. (1996). The 3′UTR of CaMKIIα mRNA is a cis-acting signal for the localization and translation of mRNA in dendrites. PNAS *93*, 13250–13255.

Mori, Y., Imaizumi, K., Katayama, T., Yoneda, Y., and Tohyama, M. (2000). Two cis-acting elements in the 3′UTR of CaMKIIα regulate its dendritic targeting. Nat. Neurosci. *3*, 1079–1084.

Munro, T.P., Magee, R.J., Kidd, G.J., Carson, J.H., Barbarese, E., Smith, L.M., and Smith, R. (1999). Mutational analysis of a heterogeneous nuclear ribonucleoprotein A2 response element for RNA trafficking. J. Biol. Chem. *274*, 34389–34395.

Okabe, S., and Hirokawa, N. (1991). Actin dynamics in growth cones. J. Neurosci. *11*, 1918–1929.

Okada, K., Soda, E.A., and Bamburg, J.R. (2000). Regulating actin dynamics in neuronal growth cones. J. Neurobiol. *44*, 126–144.

Paves, H., and Saarma, M. (1997). Neurotrophins as in vitro guidance molecules for embryonic sensory neurons. Cell Tissue Res. *290*, 285–297.

Rehbein, M., Kindler, S., Horke, S., Horke, S., and Richter, D. (2000). Two trans-acting rat-brain proteins, MARTA1 and MARTA2, interact specifically with the dendritic targeting elment in MAP2 mRNAs. Mol. Brain Res. *79*, 192–201.

Rook, M.S., Lu, M., and Kosik, K.S. (2000). CaMKIIα 3′UTR directed mRNA translocation in living neurons: visualization by GFP linkage. J. Neurosci. *20*, 6385–6393.

Ross, A., Oleynikov, Y., Kislauskis, E., Taneja, K., and Singer, R. (1997). Characterization of a β-Actin mRNA zipcode-binding protein. Mol. Cell. Biol. *17*, 2158–2165.

Schnorrer, F., Bohman, K., and Nusslein-Volhard, C. (2000). The molecular motor dynein is involved in targeting Swallow and bicoid RNA to the anterior pole of Drosophila oocytes. Nat. Cell Biol. *2*, 185–190.

Shen, K., and Meyer, T. (1999). Dynamic control of CaMKII translocation and localization in hippocampal neurons by NMDA receptor stimulation. Science *284*, 162–166.

Shestakova, E., Singer, R.H., and Condeelis, J. (2001). The physiological significance of β-actin mRNA localization in determining cell polarity and directional motility. Proc. Natl. Acad. Sci. USA *98*, 7045–7050.

Shuster, C.B., and Herman, I.M. (1995). Indirect association of ezrin with F-actin: isoform specificity and calcium sensitivity. J. Cell Biol. *128*, 837–848.

Steward, O., and Schuman, E.M. (2001). Protein synthesis at synaptic sites on dendrites. Annu. Rev. Neurosci. *24*, 299–325.

Sundell, C.L., and Singer, R.H. (1991). Requirement of microfilaments in sorting of actin mRNAs. Science *253*, 1275–1277.

Tiedge, H., and Brosius, J. (1996). Translational machinery in dendrites of hippocampal neurons in culture. J. Neurosci. *16*, 7171–7181.

Tiedge, H., Bloom, F.E., and Richter, D. (1999). RNA, whither goest thou. Science *283*, 186–188.

Wilkie, G., and Davis, I. (2001). *Drosophila wingless* and pair-rule transcripts localize apically by dynein-mediated transport of RNA particles. Cell *105*, 209–219.

Yisraeli, J.K., Sokol, S., and Melton, D.A. (1990). A two-step model for the localization of maternal mRNA in Xenopus oocytes: involvement of microtubules and microfilaments in the translocation and anchoring of Vg1 mRNA. Development *108*, 289–298.

Zhang, H.L., Singer, R.H., and Bassell, G.J. (1999a). Neurotrophin regulation of beta-actin mRNA and protein localization within growth cones. J. Cell Biol. *147*, 59–70.

Zhang, J.Y., Chan, E.K., Peng, X.X., and Tan, E.M. (1999b). A novel cytoplasmic protein with RNA binding motifs is an autoantigen in human hepatocellular carcinoma. J. Exp. Med. *189*, 1101–1110.

Zhang, Q., Yaniv, K., Oberman, F., Wolke, U., Git, A., Fromer, M., Taylor, W.L., Meyer, D., Standart, N., Raz, E., and Yisraeli, J.K. (1999c). Vg1 RBP distribution and evolutionarily conserved expression at multiple stages during development. Mech. Dev. *88*, 101–106.